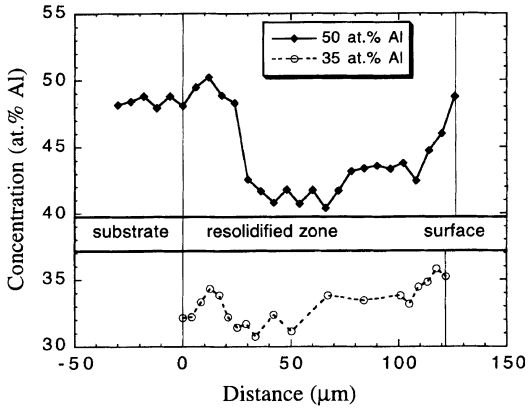

FIG. 4 The composition profiles (measured by EDS) along a trace on the cross-section of the resolidified zone in the pulsed-laser-treated samples with nominal compositions of 35 and 50 at.% Al. The decrease in the average aluminium content of the resolidified zone is an indication of aluminium loss, possibly due to evaporation. However, the rise of aluminium concentration near the surface of both samples indicates solute partitioning by rejection of aluminium into the liquid at the later stages of regrowth.

laser treatments, the resolidified zones were sliced perpendicular to the treated surface. The cross-sections of resolidified zones were initially examined by optical metallography; no dendritic structure was observed. Energy- dispersive spectrometry (EDS) along a trace on the sections (Fig. 4) confirms that there is significant compositional inhomogeneity in both samples as a result of rapid solidification. The decrease of the average aluminium content of the resolidified zones (especially in the NiAl sample with 50 at.% Al) indicates the possible loss of aluminium due to evaporation. Both profiles show a local maximum in the resolidified region near the substrate. This initial rise in the aluminium content can be interpreted as follows. The initial growth velocity in the region near the substrate, where non-equilibrium effects are negligible, is expected to be relatively low. Therefore, according to the equilibrium phase diagram (Fig. 2), the initial solid growing into a nickel-rich (B-rich) liquid would contain more Al than the liquid. However, as solidification proceeds, the interface accelerates and the non-equilibrium effects emerge. The solid grows into a liquid which is even more enriched in Ni, owing to the evaporation of Al. These two factors may explain the subsequent drop in the Al concentration. But the most important result is the rise in the Al content of the solid near the surface (the right of both composition profiles) indicating the rejection of Al into the liquid during regrowth; this could happen only if the partitioning had inverted (as in Fig. 3*c*). As shown by the two composition profiles, overall loss of Al does not affect the (predicted or observed) direction of the partitioning. Indirectly, the experiments provide evidence that rapid solidification can induce chemical disorder even in NiAl, for which the disordered state cannot readily be retained[8]. The disordered state persists only in a transient layer behind the solid–liquid interface, but has profound effects on partitioning.

These findings emphasise the differences in the solidification behaviour between ordered and disordered phases due to the energetic effects of site-ordering. In particular, there is the unprecedented demonstration that rapid growth may result not in reduced partitioning—always regarded as an advantage of rapid solidification processes—but in increased partitioning. Such an increase in partitioning may lead to the appearance of second phases and is likely to be a problem in welding and surface treatments of intermetallic compounds. On the other hand, the existence of a zero-partitioning point (for example I in Fig. 3) may be of use in producing chemically uniform intermetallic compounds where significant segregation would normally be expected.

A detailed kinetic analysis of the solidification of the ordered phase in this model system, or of γ' phase in the NiAl system[9], shows that the inversion of partitioning can, for certain values of growth velocity and composition, be associated with the liquidus temperature falling below that of the solidus; in this case there is 'solutal superheating' (as opposed to 'solutal undercooling' which makes the interface morphologically unstable[10], and absolute stability of the solid–liquid interface in a way essentially different from that due to capillarity effects[11]. Again, this is of practical relevance as planar-front solidification is often desirable in the directional solidification of intermetallic compounds, but may be difficult to achieve in these systems with high thermal conductivity.

It follows from modelling and experiment that the reliable analysis of solidification in systems in which the major constituent is a compound will be possible only if account is taken of the chemical-order effects. □

Received 7 March; accepted 23 July 1996.

1. Chalmers, B. *Principles of Solidification* 126 (Wiley, New York, 1964).
2. Smith, P. M. & Aziz, M. J. *Acta Metall. Mater.* **42,** 3515–3525 (1994).
3. Kar, A. & Mazumder, J. *Acta Metall. Mater.* **40,** 1873–1881 (1992).
4. Assadi, H. & Greer, A. L. *Mater. Res. Soc. Symp. Proc.* (in the press).
5. Boettinger, W. J. & Aziz, M. J. *Acta Metall.* **37,** 3379–3391 (1989).
6. West, J. A., Manos, J. T. & Aziz, M. J. *Mater. Res. Soc. Symp. Proc.* **213,** 859–864 (1991).
7. Aziz, M. J. *J. Appl. Phys.* **53,** 1158–1168 (1982).
8. Koch, C. C. *Int. Mater. Rev.* **33,** 201–219 (1988).
9. Assadi, H. & Greer, A. L. *Iron Steel Inst. Jpn Int.* **35,** 574–579 (1995).
10. Tiller, W. A., Jackson, K. A., Rutter, J. W. & Chalmers, B. *Acta Metall.* **1,** 428–437 (1953).
11. Mullins, W. W. & Sekerka, R. F. *J. Appl. Phys.* **34,** 444–451 (1964).

ACKNOWLEDGEMENTS. We thank R. W. Cahn and J. M. Robinson for provision of samples and experimental assistance.

CORRESPONDENCE should be addressed to A.L.G. (e-mail: alg13@cam.ac.uk).

Recent changes in tropical freezing heights and the role of sea surface temperature

Henry F. Diaz* & Nicholas E. Graham†

* NOAA/ERL/CDC, 325 Broadway, Boulder, Colorado 80303, USA
† Climate Research Division, Scripps Institution of Oceanography, La Jolla, California 92093, USA

A WIDESPREAD retreat of alpine glaciers[1] and melting of tropical ice-cap margins[2–7] has been observed in recent decades, over which time a general climate warming at lower altitudes has been documented[8]. Moreover, some ice-core records provide evidence suggesting that mid-tropospheric temperatures in the tropics have been greater in recent decades than at any time during the past 2,000–3,000 years[7]. Here we examine the processes controlling mountain glacier retreat by comparing high-altitude air-temperature measurements for the past few decades, to the temperatures predicted by a model atmosphere forced by the observed global pattern of sea surface temperature in a 19-year simulation[9]. The comparison strongly indicates that the observed changes in freezing-level height (the altitude of the 0 °C isotherm) are related to a long-term (over decades) increase in sea surface temperature in the tropics, and the consequent enhancement of the tropical hydrological cycle. Although changes in this cycle are likely to affect high-elevation hydrological and ecological balances worldwide[10,11], tropical environments may be particularly sensitive because the changes in tropical sea surface temperature and humidity may be largest and most systematic at low latitudes.

Some recent studies of high-elevation records in Europe[12,13] have shown that surface air temperature measured at several isolated mountain peaks has risen by more than 1 °C during the

past century. The inferred warming is consistent with oxygen isotopic changes ($\delta^{18}O$) which indicate warming in the past 100 years, with the greatest change occurring in the past few decades[7]. Although such isotopic records are open to various interpretations, the implied temperature record is largely consistent with similar records constructed from sea surface temperatures (SST) and air-temperature records on land[8,14]. Furthermore, there is clear evidence[15] from at least one tropical glacier than extensive surface melting occurred sometime during the past two decades, for the first time in several hundred years. Other studies[16–18] have documented upward trends in tropical tropospheric temperature and moisture content in recent decades[16–18].

Here we compare the observed changes in freezing-level heights, derived from radiosonde measurements in the tropics, to those obtained using the results of a numerical model simulation of the atmospheric response to observed SST in the period 1970–88. Further comparison of the temperature changes in high-elevation environments is made by using 40–45 years of surface temperature records from weather stations situated above 1,000 m in elevation, and vertical temperature profiles from about 75 radiosonde stations[18,19] in the tropics (the region from 30° N to 30° S).

The numerical simulations were performed with the ECHAM2 and ECHAM3 climate models (Max Planck Institute) configured to give spatial resolution of approximately 5.5° and 2.8° latitude (T21 and T42 spectral truncations). Nineteen-year climate simulations, with prescribed global observed SST for the period 1970–88, were conducted with each model[9]. Two sets of radiosonde data were used to evaluate the modelling results: a set of 65 radiosonde stations distributed throughout the tropics from about 30° N to 30° S, with data available for the period 1970–86, and a second set of 10 stations in South America[19], with a longer record (1958–90) which were situated mainly in a meridional direction. The air-temperature observations from the 12:00 GMT daily soundings (except for Lima in Peru, where only the 00:00 GMT soundings were available) were used to estimate the geopotential height of the local freezing surface by simple linear interpolation between the two levels straddling the 0 °C air-temperature value. The data contained information at significant level heights, as well as at the standard pressure levels. The monthly mean height of the 0 °C surface was calculated by averaging the calculated, daily freezing-level heights.

Figure 1 shows the evolution of the freezing-level surface (FLS) anomalies (in each instance, the mean over the period of record for each calendar month was removed) averaged over the tropics (30° N–30° S) in the T21 and T42 model runs (the heavy solid and heavy dashed curves, respectively), together with the corresponding value (thin solid line) obtained by averaging the values from the data from the 65 radiosonde stations binned into 5° latitude bands. The temporal increase of the freezing-level height from 1970 to the late 1980s, in the deep tropics (~15° N–15° S), amounts to about 110 m (calculated from the total linear trend over the analysis period). A latitude profile comparison of the simulated annual-mean freezing-level height changes, for the two models, is given in Fig. 2. For comparison, the equivalent changes based on the radiosonde data are shown by large filled circles. The patterns are quite similar, but the magnitude of the changes in the T42 run is greater, and both simulations may underestimate the observed changes in FLS in the deep tropics (~10° N–10° S). There are substantial differences between the model results and the observations, at latitudes less than about 10° N, which reflect, at least in part, sampling differences between them. There are also seasonal differences (not shown) in FLS height which are evident in the simulation, but the critical feature is the general increase of FLS height in the tropics during this time. The spatial detail of the T42 simulation is more realistic and is the one considered below.

Figure 3 illustrates the spatial distribution of annual mean FLS changes in the T42 model simulation, which indicates that the pattern of freezing-level height changes in the model strongly resembles the upper-tropospheric anomaly pattern which occurs during the course of El Niño events in the tropical Pacific Ocean[20,21]. Some of the greatest simulated warming occurs in the region of Peru where both the Quelccaya and Huascarán ice caps[2,7] are located (see Fig. 3). The question is whether this mid-tropospheric warming is associated with the recent ~20-yr episode of generally above average SST in the tropical Pacific[9,22–24]. One of the studies[9] of this episode, a synthesis of observational and model data, provides evidence indicating that the increases in tropical SST during this period result in an enhancement of the tropical hydrological cycle. One manifestation of such an enhancement is a trend towards larger temperature increases with height in the tropical troposphere. This is a consequence of a tendency for the vertical temperature structure to approach more closely a moist, adiabatic lapse-rate.

A further test of the SST–FLS link is shown in Fig. 4. The annual mean changes in FLS, for the set of 10 long-term radiosonde stations in South America, are depicted here in the form of box plots which represent the distribution of anomalous FLS height for each year, among the 10 South American radiosonde stations. There is a notable jump in FLS heights which occurs around 1976–77. Because tropical SST changes in the 1970s have been implicated in a variety of anomalous geophysical events[24], we compare the observed changes in tropical SST, from the late 1950s to 1990, to the corresponding changes in FLS in South America

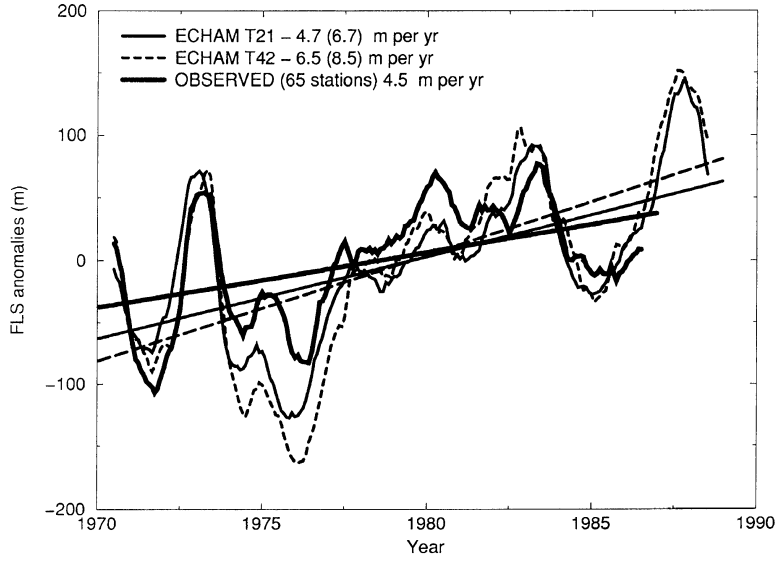

FIG. 1 Anomaly time series of the average height (in metres) of the 0 °C surface (the FLS) in the tropics (1970–88), derived from the ECHAM2–T21 and ECHAM2–T42 simulation as described in the text. Also shown is the equivalent change in freezing-level height from a network of 65 radiosonde stations located from 30° N to 30° S for the period 1970–86. Linear trends of 4.7 and 6.5 m yr^{-1} for FLS height in the T21 and T42 simulations are for the period 1970–86. The values in parentheses (6.7 and 8.5 m yr^{-1} for T21 and T42, respectively) are for 1970–88.

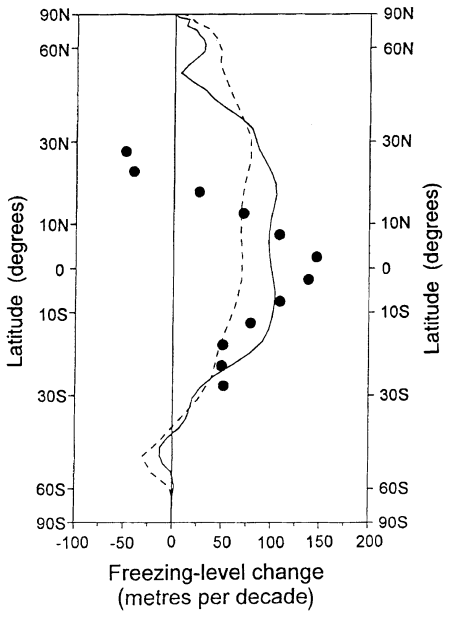

FIG. 2 A comparison of the total linear trends (in metres) of the annual mean freezing-level heights, in an 18 yr global climate model (GCM) simulation with the T21 (dashed line) and T42 ECHAM2 models, as a function of latitude, with the corresponding changes in the observations (solid dots). The linear trend changes for the radiosonde data (1970–86) were binned into 5° boxes and the median value within each 5° band was plotted.

(Fig. 4, smooth solid line). To underline the connection between the changes in the hydrological cycle in the Pacific region and the SST and FLS height, an index of the precipitation changes in the tropical Pacific[25] is also shown (smooth dotted line). The results in Fig. 4 suggest a fairly tight coupling of the tropical SST (arising mostly from changes in the tropical Pacific Ocean), rainfall changes in the Pacific and the freezing-level heights over South America. The rainfall variations are large and strongly influenced by the El Niño/Southern Oscillation phenomenon[25]. However, the relative changes between all the variables are consistent over time.

One further observational test was performed to address the latitudinal representativeness of the changes found in the radiosonde data. We have calculated linear (surface) temperature trends for a longer period of temperature observations (1951–94) using all available data from stations situated more than 1,000 m above sea level. The station data are part of the US National Climatic Data Center archives and were binned into 20°-bands from 30° S to 30° N, with a fourth band made up of all available stations located at latitudes greater than 30° N. The resulting temperature trends are consistent with the changes in FLS height derived from the set of radiosonde observations described above, and the modelling experiments (Fig. 2). That is, surface air-temperatures in higher elevation (>1,000 m) tropical regions have risen by a few tenths of a degree Celsius since about 1950, and there is some indication that the changes are greater in magnitude than the corresponding changes in the extratropics, which are only marginally positive during this period.

Our analysis provides evidence for a rise in tropical freezing-level surface elevation that is closely coupled to increases in tropical SST during the past few decades. This change is consistent with the observations of the melting of high-elevation tropical ice

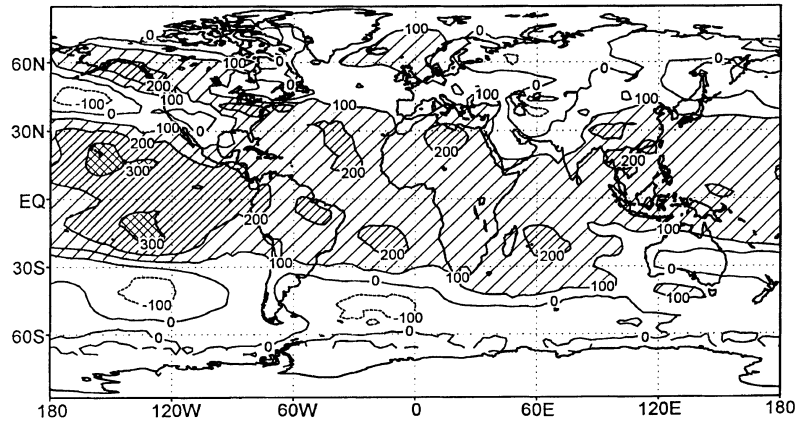

FIG. 3 A comparison of the spatial distribution of the total linear trends (in metres) in annual mean freezing-level heights in an 18-yr GCM simulation with the ECHAM3–T42 model version.

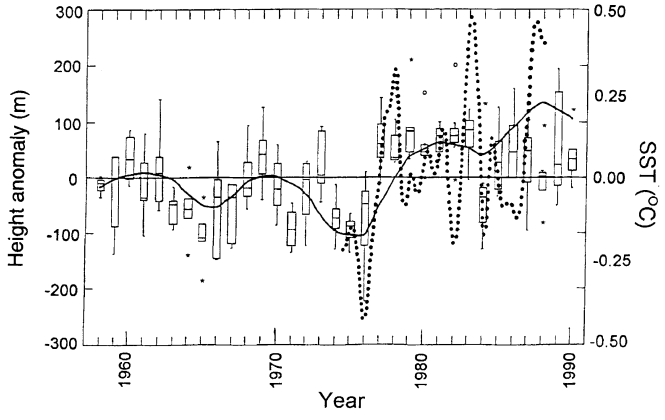

FIG. 4 Distribution of annual freezing-level height anomalies for 10 radiosonde stations in South America for the period 1958–90. The results are presented in terms of 'box and whisker' plots, which show approximately the 5th, 25th, 50th and 95th percentiles of the FLS height anomaly with respect to the station means, and values falling outside these limits, indicated by asterisks or open circles (99th percentile). The stations used were: Bogota, Colombia; Manaus, Brazil; Lima, Peru; La Paz, Bolivia; Antofagasta, Quintero, Puerto Montt and Punta Arenas, Chile; Salta and Rio Grande, Argentina. The smoothed solid line represents the low-pass filtered, median tropical SST anomalies (seasonal values referenced to the 1951–92 period) based on a 5° gridded dataset, and the solid dots correspond to the time coefficients (arbitrary units, scaled to the SST axis) of the first principal component of tropical Pacific annual mean rainfall[25].

in the Andes. Although changes in temperature are probably the dominant mechanism which produces this melting, there is also evidence, from both observations and models, that the changes in temperature have been accompanied by increases in moisture content in the lower tropopopsphere[17,18], which is consistent with the increase of the tropical SST and the resulting enhancement of the tropical hydrological cycle. These increases in humidity would also contribute to accelerated melting rates[4].

On the basis of very long isotopic records obtained from the various tropical ice-cap cores (of the order of several centuries to several thousand years), the warmth recorded in the tropical oceans in several past decades may perhaps be at an unprecedented level since the mid-Holocene period (~3,000–4,000 yr BP)[7]. Whether this recent increase is natural, anthropogenic, or both, remains an open question. Recent evidence[1,11], however, suggests that high-elevation environments may be particularly sensitive to long-term changes in tropical SST and tropospheric humidity, which are likely to have an impact on the hydrological and ecological balances of high-altitude zones throughout the globe, perhaps to the greatest extent in the tropics. □

Received 6 March; accepted 23 July 1996.

1. Oerlemans, J. *Science* **264,** 243–245 (1994).
2. Thompson, L. G. *et al. Globl Planet. Change* **7,** 145–156 (1993).
3. Brecher, H. H. & Thompson, L. G. *Photogramm. Eng. Remote Sensing* **59,** 1017–1022 (1993).
4. Hastenrath, S. & Kruss, P. *Ann. Glaciol.* **16,** 127–133 (1992).
5. Kaser, G. & Noggler, B. *J. Glaciol.* **37,** 315–318.
6. Schubert, C. *Erdkunde* **46,** 58–64 (1992).
7. Thompson, L. G. *et al. Science* **269,** 46–50 (1995).
8. Intergovernmental Panel on Climate Change (IPCC) *Climate Change'95, The Science of Climate Change* (Cambridge Univ. Press, 1996).
9. Graham, N. E. *Science* **267,** 666–671 (1995).
10. Schneider, S. H. *Bull. Am. Meteorol. Soc.* **71,** 1292–1304 (1990).
11. Beniston, M. (ed.) *Mountain Environments in Changing Climates* (Routledge, London, 1994).
12. Beniston, M., Rebetez, M., Giorgi, F. & Marinucci, R. *Theor. Appl. Climatol.* **49,** 135–159 (1994).
13. Weber, R. O., Talkner, P. & Stefanski, G. *Geophys. Res. Lett.* **21,** 673–676 (1994).
14. Jones, P. D., Bradley, R. S. & Jouzel, J. (eds) *Climatic Variations and Forcing Mechanisms of the Last 2000 Years* (NATO ASI Series, Springer, Berlin, 1996).
15. Thompson, L. G. *Melting of our Tropical Climatic Archives* (PAGES Core Project Office, Bern, Switzerland, 1995).
16. Hense, A. P., Krahe, P. & Flohn, H. *Meteorol. Atmos. Phys.* **38,** 215–227 (1988).
17. Gutzler, D. S. *Geophys. Res. Lett.* **19,** 1595–1598 (1992).
18. Gaffen, D. J., Barnett, T. P. & Elliott, W. P. *J. Clim.* **4,** 989–1008 (1991).
19. Eskridge, R. E. *et al. Bull. Am. Meteorol. Soc.* **76,** 1759–1775 (1995).
20. Newell, R. E. & Wu, Z.-X. *J. Geophys. Res.* **97,** 3693–3709 (1992).
21. Yulaeva, E. & Wallace, J. M. *J. Clim.* **7,** 1719–1736 (1994).
22. Trenberth, K. E. *Bull. Am. Meteorol. Soc.* **71,** 998–993 (1991).
23. Graham, N. E. *Clim. Dyn.* **10,** 135–162 (1994).
24. Miller, A. J., Cayan, D. R., Barnett, T. P., Graham, N. E. & Oberhuber, J. M. *Oceanogr.* **7,** 21–26 (1994).
25. Morrissey, M. L. & Graham, N. E. *Bull. Am. Meteorol. Soc.* **77,** 1207–1219 (1996).

ACKNOWLEDGEMENTS. This work was partially supported by the US Department of Energy and the US National Oceanic and Atmospheric Administration. It grew out of discussions at a meeting in Wengen, Switzerland in September 1995 which was funded by several US and European agencies and organized by H.F.D. and M. Beniston of the Swiss Institute of Technology (ETH) in Zürich. We thank M. Beniston, R. Bradley, S. Hstenrath, J. Hurrell, U. Schotterer and L. Thompson for discussion, L. Bengtsson and E. Roeckner for providing the results form the MPI models, and T. Barnett and D. Gaffen for providing the 65 station radiosonde dataset.

CORRESPONDENCE should be addressed to H.F.D. (e-mail: hfd@cdc.noaa.gov).

Microbial generation of economic accumulations of methane within a shallow organic-rich shale

Anna M. Martini*, Joyce M. Budai*, Lynn M. Walter* & Martin Schoell†

* Department of Geological Sciences, University of Michigan, 2534 C C Little Building, 425 East University, Ann Arbor, Michigan 48109-1063, USA
† Chevron Petroleum Technology Company, 1300 Beach Boulevard, La Habra, California 90631, USA

ALTHOUGH **methane of bacterial origin is ubiquitous in marine and freshwater sediments, economic accumulations of bacterial gases occur mainly at depths of several kilometres in Tertiary basins that had high sedimentation rates[1,2]. Here we present an integration of geochemical and isotopic data from gas and water extracted from the Upper Devonian Antrim shale, along the northern margin of the Michigan basin, which demonstrates that significant volumes of bacterial gas have been generated in organic-rich shales at depths of less than 600 metres. The Antrim shale is mainly a self-sourced reservoir, in contrast to conventional gas deposits that have migrated from a source to a reservoir, and has become one of the most actively exploited gas reservoirs[3] in the United States. The gas-forming processes operating at shallow depths in the Antrim shale are not unique[4], and an understanding of these processes should lead to the identification and development of other economic, non-conventional gas deposits around the world.**

The Antrim shale is rich in organic matter (up to 20 wt%), comprised of hydrogen-rich algal material and is thermally immature (vitrinite reflectance $R_o = 0.4–0.6$) in the area of study[5]. Our study area is along the northern margin of the Michigan basin

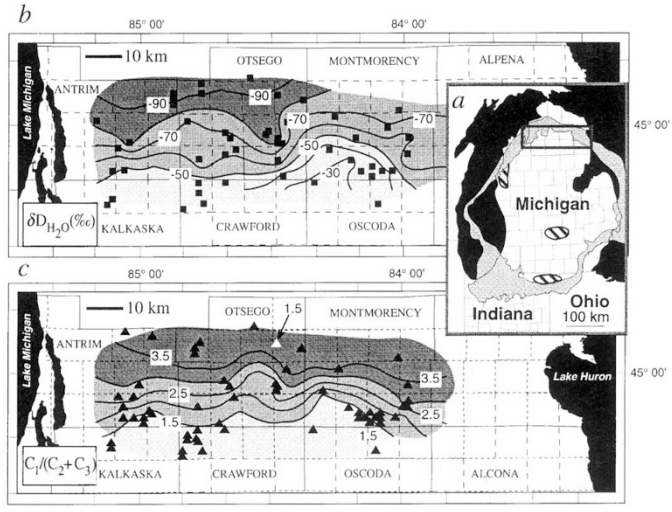

FIG. 1 *a*, Study area at the margin of the Michigan basin in northern Michigan, USA with the subcrop of the Antrim shale shown in grey. Over 5,000 wells have been completed in the shale for commercial production of methane. Of these, over 95% were commercially successful. Estimates[3] of total Antrim shale reserves for the Michigan basin are in the range $(9–29) \times 10^{11}\,m^3$. Gas and co-produced water were collected at the well-head. Sampling depths ranged from 200 m on the northern margin of the producing zone, to nearly 650 m in the south. Striped areas indicate regions of new exploration. *b*, Gradients in δD values of water (shown on contours) occur over the producing trend due to freshwater ($\delta D \approx -90‰$) influx mixing with basinal brines ($\delta D \approx -30‰$). Well locations are shown as filled squares. The δD value of the water was determined using a Finnigan MAT Delta S ratio mass spectrometer, with a precision of ±2‰. Waters were reacted with zinc metal to liberate hydrogen gas[28]. *c*, A plot of $\log(C_1/(C_2 + C_3))$ for produced gas from the Antrim shale, showing a steep gas compositional gradient (with increasing C_{2+} content) from the margin towards the centre of the basin. The value for one anomalous well (shown as an open triangle) is not contoured as contamination is suspected. Gas samples were obtained from the well-head using stainless-steel cylinders, and analysed by routine gas chromatographic techniques.